AGU ADVANCING EARTH AND SPACE SCIENCE

Geophysical Research Letters®

RESEARCH LETTER
10.1029/2022GL099959

Key Points:

- Thallium isotope compositions of the alkaline rocks were analyzed to track crustal recycling in the subcontinental lithospheric mantle
- Thallium isotope suggested that low-temperature altered oceanic crust and pelagic sediments were not involved in the investigated sources
- The O-Nd-Hf-Tl isotope data for the Liaodong-Jinan volcanics reveal a significant Tl-loss in the subducted slab during dehydration process

Supporting Information:

Supporting Information may be found in the online version of this article.

Correspondence to:

X. Chen,
xchen6@sjtu.edu.cn;
blueskybluedreams@gmail.com

Citation:

Mei, Q.-F., Chen, X., Yang, J.-H., Zhu, Y.-S., & Owens, J. D. (2022). Tracing recycled crustal materials in the subcontinental lithospheric mantle using Thallium isotopes. *Geophysical Research Letters*, *49*, e2022GL099959. https://doi.org/10.1029/2022GL099959

Received 11 JUN 2022
Accepted 25 JUL 2022

Author Contributions:

Conceptualization: Qing-Feng Mei, Xinming Chen
Data curation: Qing-Feng Mei, Xinming Chen
Formal analysis: Qing-Feng Mei, Xinming Chen
Funding acquisition: Qing-Feng Mei, Jin-Hui Yang, Jeremy D. Owens
Investigation: Qing-Feng Mei, Xinming Chen
Methodology: Xinming Chen, Jeremy D. Owens
Resources: Jin-Hui Yang
Validation: Qing-Feng Mei, Xinming Chen
Visualization: Qing-Feng Mei, Xinming Chen

Tracing Recycled Crustal Materials in the Subcontinental Lithospheric Mantle Using Thallium Isotopes

Qing-Feng Mei[1], Xinming Chen[2,3], Jin-Hui Yang[1], Yu-Sheng Zhu[1], and Jeremy D. Owens[3]

[1]State Key Laboratory of Lithospheric Evolution, Institute of Geology and Geophysics, Chinese Academy of Sciences, Beijing, China, [2]School of Oceanography, Shanghai Jiao Tong University, Shanghai, China, [3]National High Magnetic Field Laboratory and Department of Earth, Ocean & Atmospheric Science, Florida State University, Tallahassee, FL, USA

Abstract Here we report the first set of thallium (Tl) isotope data in alkaline rocks from the North China Craton to constrain the nature of recycled materials in the metasomatized subcontinental lithospheric mantle. Samples from the Hekanzi and Saima alkaline complexes display Tl isotope compositions (ε^{205}Tl) identical to the present-day upper mantle and continental crust, suggesting that neither the recycled low-temperature altered oceanic crust nor the pelagic sediments were involved in their sources. The volcanic rocks from the Liaodong-Jinan region, whose source was previously proposed to contain recycled low-temperature altered oceanic crust, also display modern mantle-like Tl isotope composition, suggesting a significant Tl-loss in the recycled oceanic crust during the subduction due to the dehydration process. Our Tl isotope data provide complementary constraints to the Sr-Nd-Hf-O isotopes on the nature of metasomatic agent in the subcontinental lithospheric mantle.

Plain Language Summary Recycling of crustal materials into Earth's mantle by subduction causes mantle heterogeneities. The sources of some alkaline rocks contain recycled crustal materials. Pelagic sediments, low-temperature altered oceanic crust, and continental crust have sharp differences in thallium isotope compositions. Combined with Sr-Nd-Hf-O isotopes, whole-rock Tl isotopes place a better constraint on the metasomatic sources.

1. Introduction

According to the crust-mantle differentiation theory, the subcontinental lithospheric mantle (SCLM) should be depleted in incompatible elements because of the crust-forming melt extraction (Jordan, 1978). However, the SCLM can be subsequently metasomatized by the melts and/or fluids (metasomatic agents) and therefore re-enriched in fusible elements. Metasomatism in SCLM can lead to lithospheric thinning coupled with a series of surface responses (e.g., intraplate magmatism, tectonism, and mineralization) and occasionally trigger craton destruction (e.g., Foley, 2008; Gao et al., 2004; Wu et al., 2019; Xu, 2001; Zhu et al., 2017). The metasomatic agents are likely derived from the underlying asthenosphere mantle, or subducted oceanic crust with pelagic sediments, or recycled continental crust (e.g., Coltorti et al., 2000; Prouteau et al., 2001; Tappe et al., 2013; Y. F. Zheng, 2012; Zhu et al., 2017). Identifying the exact source of metasomatic agents can build the linkages between magmatism and tectonics, reveal the genetic mechanism in the deep mantle accounting for the surface responses, and further reconstruct the geological history of studied areas.

Radiogenic Sr-Nd-Hf-Pb isotopes are commonly employed to trace the recycled crustal materials in the metasomatic agent. However, they are strongly affected by the residence time of the source components and elemental fractionation during magma evolution (e.g., Nielsen et al., 2007; Prytulak et al., 2017). Stable isotopes have the potential to avoid these disadvantages and record low-temperature processes that impart isotope fractionation, thus providing complementary insights into the nature of the metasomatic agent. Thallium isotopes ($\varepsilon^{205}\text{Tl} = [(^{205}\text{Tl}/^{203}\text{Tl})_{\text{sample}}/(^{205}\text{Tl}/^{203}\text{Tl})_{\text{NIST SRM 997}} - 1] \times 10^4$) are a promising tool to discern recycled crustal materials and pelagic sediments in metasomatic agents, given the sharp contrasts in Tl abundance and isotope composition in pelagic sediments, low-temperature altered oceanic crust (low-T AOC), and the mantle. Specifically, Tl is significantly enriched in low-T AOC, pelagic sediments, and continental crust (~10–1000, >1000, and ~500 ng/g) compared with the mantle (~0.5 ng/g) (Nielsen et al., 2014; Nielsen, Rehkämper, & Prytulak, 2017; Rudnick & Gao, 2003). Low-T AOC and pelagic sediments document the most negative and positive ε^{205}Tl values (~−16 and ~+15), while the mantle value of ε^{205}Tl is −2.0 ± 0.5 (e.g., Nielsen, Rehkämper, Norman,

Writing – review & editing: Qing-Feng Mei, Xinming Chen, Jin-Hui Yang, Yu-Sheng Zhu, Jeremy D. Owens

et al., 2006; Nielsen, Rehkämper, Teagle, et al., 2006; Rehkämper et al., 2004). More importantly, Tl isotopes appear only minorly affected by partial melting and fractional crystallization processes, which gives Tl isotopes another advantage in their applications in mantle geochemistry (Aarons et al., 2021; Baker et al., 2010; Gaschnig et al., 2021; Nielsen, Prytulak, et al., 2017; Nielsen, Rehkämper, Norman, et al., 2006; Prytulak et al., 2017; Rader et al., 2021). As a result, Tl isotopes are being widely explored to trace recycled materials in subduction zones (e.g., Nielsen et al., 2015, 2016; Nielsen, Prytulak, et al., 2017; Shu et al., 2017). Here, we measured whole-rock ε^{205}Tl of Mesozoic alkaline rocks from three localities (Hekanzi, Saima, and Liaodong-Jinan) in the North China Craton (NCC) to extend the application of Tl isotopes to trace the recycled crustal materials in the metasomatized SCLM and improve the understanding of Tl cycle of the Earth in the geological history.

2. Geological Setting

The NCC, the Chinese portion of the Sino-Korean Craton, is bounded to the north by the Central Asian Orogenic Belt, and to the southwest and southeast by the Qinling-Dabie-Sulu Orogenic Belt (Wang & Mo, 1995) (Figure S1 in Supporting Information S1). Cratonization of the NCC occurred at ~1.9 Ga through the assembly of the eastern and western blocks (Zhao et al., 2005). The NCC was stable until the Mesozoic, during which it experienced extensive magmatism and strong tectonism, indicating craton destruction or decratonization (e.g., Wu et al., 2019; Yang et al., 2008). The magmatism of the NCC over the Phanerozoic was controlled by three events: (a) closure of the paleo-Asian Ocean (by the Xing'an Mongolian Orogenic Belt, the eastern part of the Central Asian Orogenic Belt), (b) subduction of the paleo-Tethys and subsequent northward deep subduction of the Yangtze continental crust, and (c) subduction of the paleo-Pacific Ocean plate. The last event was the primary tectonic trigger for the decratonization of the NCC (e.g., Wu et al., 2019; Yang et al., 2008, 2010).

Fifteen samples were analyzed in this study, including six syenites from the Triassic Hekanzi alkaline complex, four syenites and one trachyte (09JH67) from the Triassic Saima alkaline complex, and three trachytes as well as one trachyandesite (18JF44) from the Liaodong-Jinan (LJ) region. Zircon U-Pb dating yields emplacement ages of 226–224 Ma, 230–224 Ma, and 129–124 Ma for the Hekanzi, Saima, and LJ samples, respectively (Feng et al., 2020; Yang et al., 2012; Zhu et al., 2016). These rocks have been demonstrated to originate from low-degree partial melting of enriched SCLM (Feng et al., 2020; Yang et al., 2012; Zhu et al., 2016). The zircon Hf-O isotope data identified recycled high-temperature (high-T) AOC, continental crust, and low-T AOC in the mantle sources of Hekanzi alkaline rocks, Saima alkaline rocks, and LJ volcanic rocks, respectively (Feng et al., 2020; Zhu et al., 2017). These findings are consistent with the southward subduction of the paleo-Asian Ocean plate, the northward subduction of the Yangtze continental crust, and the subduction of the paleo-Pacific Ocean plate in the Mesozoic (Feng et al., 2020; Zhu et al., 2017).

3. Methods and Results

The sample digestion, chemical separation, and Tl isotope analyses were performed at the National High Magnetic Field Laboratory, Florida State University (MagLab, FSU), following Nielsen et al. (2004). Thallium isotopes were measured using the Thermo Finnigan Neptune multi-collector inductively coupled plasma mass spectrometer (MC-ICPMS). Thallium concentrations were calculated from the ^{205}Tl/^{208}Pb ratios measured on the MC-ICPMS due to the quantitative yields of Tl from the column chemistry procedure and the known quantity of NIST SRM 981 Pb added to the samples. The USGS basalt powder BHVO-1, processed together with the unknown samples, displayed an ε^{205}Tl value of -3.6 ± 0.4 (2SD, $N = 4$) and a Tl concentration of 37.8 ± 0.7 ng/g, consistent with previous work ($\varepsilon^{205}\text{Tl} = -3.6 \pm 0.4$; a Tl concentration of 37 ng/g; Nielsen et al., 2015; Nielsen, Rehkämper, & Prytulak, 2017; Shu et al., 2017, 2019). The long-term reproducibility of Tl isotope measurement in leached silicate samples (SCo-1) is ±0.3 ε units (2SD) at FSU (Owens, 2019).

Whole-rock Tl concentrations in samples from Hekanzi, Saima, and LJ range from 480 to 743 ng/g, from 466 to 1674 ng/g, and from 124 to 352 ng/g, respectively (Table 1). Whole-rock ε^{205}Tl values in samples from Hekanzi, Saima, and LJ vary between −2.5 and −1.3, between −3.2 and −2.2, and between −2.6 and −0.8, respectively (Table 1).

Table 1
Whole-Rock Tl and Zircon Hf-O Isotopic Data for Alkaline Rocks in This Study

Sample	Rock type	Tl (ng/g)	ε^{205}Tl	2SD	N	Ce/Tl[a]	Whole-rock $(^{87}Sr/^{86}Sr)_i$[a]	Whole-rock $\varepsilon_{Nd}(t)$[a]	Whole-rock $\varepsilon_{Hf}(t)$[a]	Zircon $\varepsilon_{Hf}(t)$[b]	2SD[b]	Zircon $\delta^{18}O$[b] (‰)	2SD[b]
Hekanzi alkaline complex													
05FW46	Pyroxene syenite	743	−1.3	0.4	3	164	0.70470	−4.7	−3.0	N.D.	N.D.	N.D.	N.D.
05FW50	Nepheline syenite	621	−2.1	0.4	3	138	0.70472	−5.8	−2.6	−1.3	1.2	4.4	0.8
05FW55	Syenite	615	−2.5	0.4	3	N.D.	0.70449	−5.9	−0.1	N.D.	N.D.	N.D.	N.D.
05FW56	Syenite	522	−2.1	0.4	3	285	0.70446	−6.5	−1.5	N.D.	N.D.	N.D.	N.D.
05FW57	Syenite	562	−1.9	0.5	4	224	0.70444	−2.4	1.2	N.D.	N.D.	N.D.	N.D.
05FW58	Syenite	480	−1.5	0.5	3	N.D.	0.70455	−5.3	−0.4	N.D.	N.D.	N.D.	N.D.
Saima alkaline complex													
09JH58	Pyroxene syenite	890	−3.2	0.4	3	303	0.70794	−12.7	−13.0	−12.5	1.0	8.0	0.6
09JH65	Amphibole syenite	1390	−3.1	0.4	3	256	0.70821	−11.8	−14.6	−13.0	1.4	7.4	0.5
09JH67	Trachyte	555	−2.4	0.4	3	537	0.70724	−12.6	−14.0	−12.3	1.4	6.7	0.4
09JH79	Nepheline syenite	466	−2.2	0.5	3	90	0.70829	−12.7	−12.0	−10.3	1.8	3.3	1.8
09JH81	Nepheline syenite	1674	−2.3	0.4	3	351	0.70825	−12.2	−12.0	−9.8	1.7	4.8	1.6
Volcanic rocks in the Liaodong-Jinan (LJ) region													
18JF10	Trachyte	232	−1.7	0.4	3	226	0.70705	−4.8	−0.9	−2.4	1.5	7.6	0.6
18JF21	Trachyte	124	−0.8	0.4	3	933	0.70672	−6.9	−8.4	−9.3	1.9	5.0	0.3
18JF24	Trachyte	318	−2.6	0.4	3	403	0.70765	−7.5	−7.5	−9.2	1.8	5.4	0.7
18JF44	Trachyandesite	352	−1.8	0.4	3	142	0.70881	−0.5	3.7	3.0	1.9	8.6	0.5

[a]Whole-rock Ce concentrations and Sr-Nd-Hf isotope data for the Hekanzi, Saima, and LJ samples are from Yang et al. (2012), Zhu et al. (2016), and Feng et al. (2020), respectively. [b]Zircon Hf-O isotope data for the Hekanzi and Saima samples are from Zhu et al. (2017); Zircon Hf-O isotope data for the LJ samples are from Feng et al. (2020).

4. Discussion

Our whole-rock Tl isotope compositions from all the measured samples are indistinguishable from the upper mantle and continental crust except one sample (-0.8 ± 0.4) from the volcanic rocks in the Liaodong-Jinan region and two samples (-3.1 ± 0.4 and -3.2 ± 0.4) from the Saima alkaline rocks. Combined with whole-rock radiogenic isotope data (Hf-Sr-Nd), we provide further constraints on the nature of recycled materials involved in the metasomatic agents of SCLM.

To identify the recycled crustal material in the sources of alkaline rocks using whole-rock Tl isotope data, it is essential to first consider petrogenetic processes such as crustal assimilation and fractional crystallization that can potentially affect Tl isotope signatures in the primary parental magma as observed for other whole-rock elemental abundance and Sr-Nd isotopes. Previous work demonstrated that the Hekanzi nepheline-bearing syenites were the result of crustal assimilation and fractional crystallization of a mafic magma derived from an amphibole-clinopyroxene-rich lithospheric mantle via low degree partial melting (Yang et al., 2012). The whole-rock Sr-Nd-Hf isotope data of these rocks define a binary mixing line between mafic magma and crustal material, indicating the process of crustal contamination (Yang et al., 2012). The mafic magma derived from SCLM has a relatively more positive $\varepsilon_{Hf}(t)$ value and lower initial $^{87}Sr/^{86}Sr$ ratio (i.e., samples 05FW55, 05FW57, and 05FW58 in Table 1) compared with those of the crustal materials, producing a negative correlation between $\varepsilon_{Hf}(t)$ and initial $^{87}Sr/^{86}Sr$ (Figure 1a). Due to the low degree partial melting in the petrogenesis of Hekanzi alkaline rocks and the high incompatibility of Tl during partial melting, the Tl concentration contrast between the mafic magma and the continental crust might be low. The primordial Tl isotope composition of the mafic component derived from the SCLM is therefore unlikely to be entirely overprinted by the continental crust during the crustal assimilation. Moreover, partial melting and fractional crystallization only impart minor Tl isotope fractionation (Baker et al., 2010; Gaschnig et al., 2021; Nielsen, Prytulak, et al., 2017; Nielsen, Rehkämper, Norman, et al., 2006; Prytulak et al., 2017). Thus, the three samples (05FW55, 05FW57, and 05FW58) least affected by

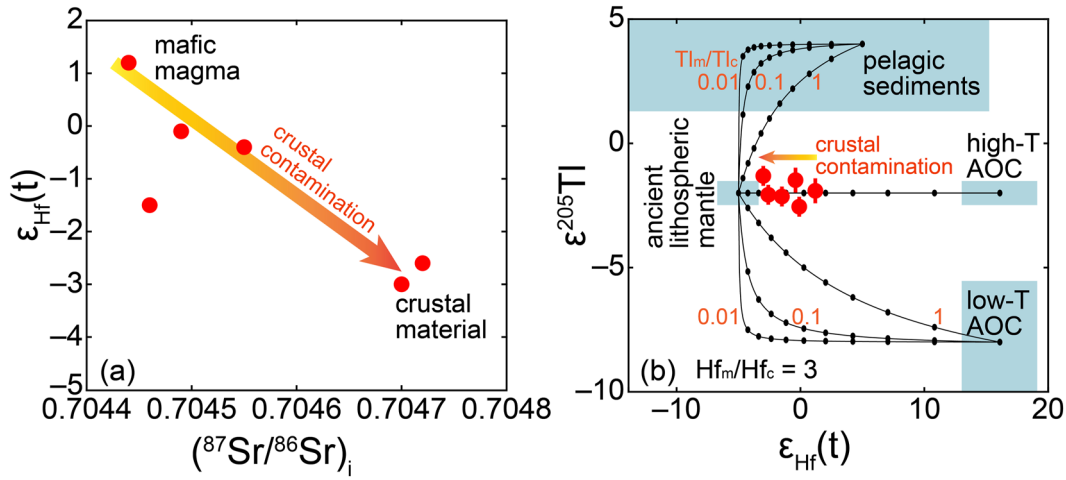

Figure 1. Whole-rock $\varepsilon_{Hf}(t)$ versus (a) the initial $^{87}Sr/^{86}Sr$ ratios and (b) the $\varepsilon^{205}Tl$ values of the Hekanzi alkaline rocks. Error bars represent 2SD. The whole-rock Hf and Sr isotope data are from Yang et al. (2012). The $\varepsilon^{205}Tl$ values of the upper mantle, high-temperature altered oceanic crust, low-temperature altered oceanic crust, and pelagic sediments (shaded areas) are from Nielsen, Rehkämper, and Prytulak (2017). The $\varepsilon_{Hf}(t)$ values of the oceanic crust are calculated from Griffin et al. (2000). The $\varepsilon_{Hf}(t)$ values of the pelagic sediments are from Vervoort et al. (2011). Superimposed on these fields are isotopic mixing curves with dots along lines that link up end members at 10% intervals. The Tl_m/Tl_c values marked beside the curves are the ratios of Tl concentrations in mantle peridotite (m) to contaminants (c). The ratio of Hf concentration of the mantle peridotite to contaminants (Hf_m/Hf_c) is 3 (Zhu et al., 2017).

crustal contamination (indicated by Hf-Sr isotope data) most likely have $\varepsilon^{205}Tl$ values that represent the primary parental magma of Hekanzi alkaline rocks.

The significantly higher whole-rock $\varepsilon_{Hf}(t)$ values (between −1.5 and + 1.2 for samples 05FW55, 05FW57, and 05FW58) in the Hekanzi samples relative to the ancient lithospheric mantle beneath the NCC ($\varepsilon_{Hf}(t) = -5$, calculated at 225 Ma; J. P. Zheng, 1999; Zhu et al., 2017) indicate that the subducted oceanic crust or the melt derived from the underlying asthenosphere mantle was likely involved in the source of Hekanzi alkaline rocks. Although our whole-rock Tl isotope data of samples least affected by crustal contamination cannot tell exactly the nature of the metasomatic agent, they can exclude the involvement of pelagic sediments and low-T AOC in the metasomatic agent. Thallium isotopes are sensitive in tracing the low-T AOC and pelagic sediments that are relevant during crustal recycling. Low-T AOC and pelagic sediments document the most negative and positive $\varepsilon^{205}Tl$ values (∼−16 and ∼ +15) due to the low-T hydrothermal alteration of oceanic crust and Tl adsorption onto authigenic Fe-Mn oxides in pelagic clays, respectively (e.g., Nielsen, Rehkämper, Norman, et al., 2006; Nielsen, Rehkämper, & Prytulak, 2017; Nielsen, Rehkämper, Teagle, et al., 2006; Rehkämper et al., 2004). The mantle-like $\varepsilon^{205}Tl$ values in samples (05FW55, 05FW57, and 05FW58) that most likely represent the mafic magma component therefore indicate that low-T AOC and pelagic sediments are unlikely to be important contributor of the Tl in the metasomatic agents for the source of the Hekanzi alkaline rocks (Figure 1b). Zircon grains crystallized from the alkaline magmas with low $\delta^{18}O$ (+3.8‰ to +5.4‰) values in the Hekanzi alkaline rocks support our interpretation because the low-T AOC and pelagic sediments are characterized by high $\delta^{18}O$ values (generally > +10‰) according to the oxygen isotope profile of altered, sediment-covered oceanic crust (Eiler, 2001; Gregory & Taylor, 1981; Zhu et al., 2017). Our whole-rock Tl isotope data provide complementary constraints to the zircon Hf-O isotope data which suggested involvement of high-T AOC in the metasomatic agents of Hekanzi alkaline rocks (Zhu et al., 2017).

Unlike the Hekanzi rocks, the Saima alkaline rocks were not significantly affected by crustal contamination. These rocks have homogeneous whole-rock $\varepsilon_{Nd}(t)$ values (between −12.7 and −11.8) and $\varepsilon_{Hf}(t)$ values (between −14.6 and −12.0) (Figure 2a). The whole-rock $\varepsilon_{Hf}(t)$ values are identical to zircon $\varepsilon_{Hf}(t)$ values in these samples (Table 1). These geochemical signatures suggest that continental crust assimilation may not play an important role in the petrogenesis of Saima rocks (Zhu et al., 2016, 2017). The whole-rock Tl isotope compositions of these rocks can therefore represent the compositions of their primary parental magma. The Saima alkaline rock also have mantle-like Tl isotopic compositions, although two samples from the Saima alkaline rocks have $\varepsilon^{205}Tl$

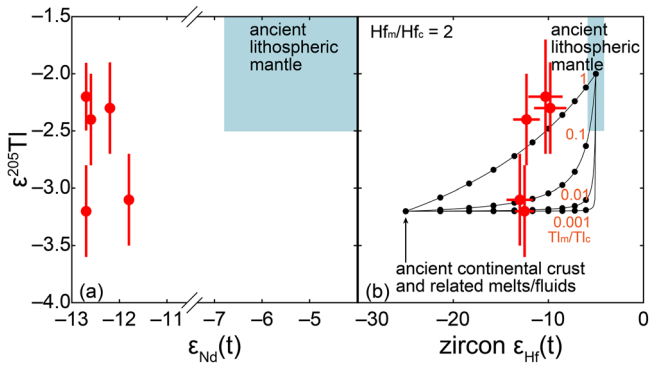

Figure 2. Whole-rock ε^{205}Tl versus (a) whole-rock $\varepsilon_{Nd}(t)$ and (b) zircon $\varepsilon_{Hf}(t)$ of the Saima alkaline rocks. The Nd and Hf isotope data are from Zhu et al. (2016, 2017). Error bars for ε^{205}Tl and $\varepsilon_{Hf}(t)$ represent 2SD. The $\varepsilon_{Hf}(t)$ value of the mantle source is −5 (Zhu et al., 2017). The $\varepsilon_{Hf}(t)$ value of the ancient continental contaminant is −25 (Yang et al., 2008; Zhu et al., 2017). The ε^{205}Tl values of the mantle source and contaminants (represented by the lowest value in Saima alkaline sample) are −2 (Nielsen, Rehkämper, & Prytulak, 2017) and −3.2, respectively. Superimposed on these fields are isotopic mixing curves with dots along lines that link up end members at 10% intervals. The Tl_m/Tl_c values marked beside the curves are the ratios of Tl concentrations in mantle peridotite (m) to contaminants (c). The ratio of Hf concentration of the mantle peridotite to contaminants (Hf_m/Hf_c) is 2 (Zhu et al., 2017).

values slightly lighter (−3.1 ± 0.4 and −3.2 ± 0.4) than the upper mantle (−2.0 ± 0.5). If we assume the slightly lighter ε^{205}Tl values result from involvement of recycled materials in the metasomatic agents, it should be low-T AOC which has significantly lighter ε^{205}Tl values (~−16) relative to the upper mantle. However, considering the tiny difference in Tl isotopic compositions and large uncertainties in ε^{205}Tl values, the low-T AOC contribution would be negligible or little. Additionally, the mantle-like ε^{205}Tl values in the other three samples also support little contribution of low-T AOC to the metasomatic agents for the source of Saima alkaline rocks. It is also unlikely that pelagic sediments, which have significantly heavier ε^{205}Tl than the upper mantle, is involved in the metasomatic agents.

The highly unradiogenic Nd and Hf isotope compositions (low $\varepsilon_{Nd}(t)$ and $\varepsilon_{Hf}(t)$ values) and the high zircon δ^{18}O values suggest that recycled ancient continental crust is most likely involved in the source of Saima alkaline rocks (Zhu et al., 2017). Figure 2b shows the variations of whole-rock ε^{205}Tl and zircon $\varepsilon_{Hf}(t)$ together with a binary mixing model between ancient lithospheric mantle and ancient continental crust. A restricted range of ε^{205}Tl values (from −3.2 to −2.2) and no evident correlation between the whole-rock ε^{205}Tl and zircon Hf isotope data indicate that the overlap of the Tl isotope compositions for the upper mantle ($\varepsilon^{205}Tl = -2.0 \pm 0.5$) and continental crust ($\varepsilon^{205}Tl = -2.0 \pm 1.0$) makes Tl isotopes difficult to be used to trace the recycled continental crust in the SCLM (Nielsen, Rehkämper, & Prytulak, 2017). However, we can at least conclude that low-T AOC or pelagic sediments make little contribution to the source of Saima alkaline rocks.

All the Early Cretaceous LJ volcanic rocks have mantle-like ε^{205}Tl values except the sample 18JF21 with a significantly heavier Tl isotopic composition of −0.8 ± 0.4 (Figure 3a). Samples that have mantle-like zircon O isotope composition (18JF21 and 18JF24) are believed to be derived from ancient lithospheric mantle (Feng et al., 2020; Valley et al., 1998). The ε^{205}Tl value of 18JF24 is −2.6 ± 0.4, indistinguishable from that of the upper mantle (−2.0 ± 0.5; Nielsen, Rehkämper, & Prytulak, 2017). In contrast, ε^{205}Tl value in sample 18JF21 (−0.8 ± 0.4) is significantly higher than the upper mantle. A possible explanation for the high ε^{205}Tl value in sample 18JF21 is the magma degassing that typically leads to significant loss of Tl as a volatile component at high temperatures and preferential loss of light Tl isotopes (e.g., Nielsen et al., 2021). The high Ce/Tl ratio of 933 in 18JF21 due to preferential loss of Tl relative to Ce during the magma degassing supports this possibility. A Tl loss of ~57% for the sample 18JF21 through the degassing under the natural gas convection could give the observed differences in ε^{205}Tl values and Ce/Tl ratios between samples 18JF24 and 18JF21 (see Figure S2 in the Supplementary information for details of the quantitative estimation of Tl loss and Tl isotope shift during degassing).

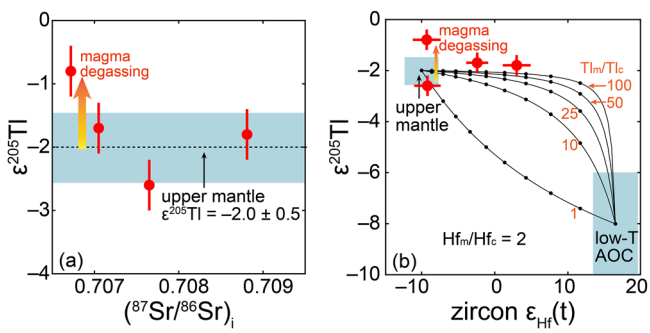

Figure 3. Whole-rock ε^{205}Tl versus (a) the initial $^{87}Sr/^{86}Sr$ ratios and (b) zircon $\varepsilon_{Hf}(t)$ of the Liaodong-Jinan alkaline rocks. Error bars represent 2SD. The whole-rock Sr isotope data and zircon Hf isotope data are from Feng et al. (2020). The ε^{205}Tl values of the upper mantle and low-temperature altered oceanic crust (shaded areas) are from Nielsen, Rehkämper, and Prytulak (2017). The $\varepsilon_{Hf}(t)$ value of the upper mantle is from Feng et al. (2020). The $\varepsilon_{Hf}(t)$ value of the low-temperature altered oceanic crust are calculated from Griffin et al. (2000). Superimposed on these fields are isotopic mixing curves with dots along lines that link up end members at 10% intervals. The Tl_m/Tl_c values marked beside the curves are the ratios of Tl concentrations in mantle peridotite (m) to contaminants (c). The ratio of Hf concentration of the mantle peridotite to contaminants (Hf_m/Hf_c) is 2 (Feng et al., 2020).

Samples 18JF10 and18JF44 have zircon δ^{18}O values of +7.6 ± 0.6‰ and +8.6 ± 0.5‰ and zircon $\varepsilon_{Hf}(t)$ values of −2.4 ± 1.5 and +3.0 ± 1.9, suggesting that their source contains materials from recycled low-T AOC (Feng et al., 2020). According to the binary mixing model in Feng et al. (2020), the inferred average δ^{18}O value for the recycled material is most likely higher than +10‰, which indicates that the recycled materials predominantly come from the portion above the sheeted dike complex of the oceanic crust cross-section (i.e., pillow basalts and pelagic sediments) (Eiler, 2001; Gregory & Taylor, 1981). The altered pillow basalt portion has ε^{205}Tl values from −2 to −16, while the pelagic sediment portion has positive ε^{205}Tl values > +2 (Nielsen et al., 2016; Nielsen, Rehkämper, Teagle, et al., 2006; Rehkämper et al., 2004). However, samples 18JF10 and18JF44 have ε^{205}Tl

values identical to the present-day upper mantle of −2. The mantle-like Tl isotope compositions in these samples therefore indicate that the source region of the Early Cretaceous LJ volcanics was not significantly affected by the Tl from low-T AOC, inconsistent with the conclusion drawn from zircon Hf-O isotopes.

The discrepancy likely results from Tl-loss due to the dehydration process during subduction of the oceanic crust. A mixing model of the upper mantle with low-T AOC (Figure 3b) suggests that the Tl_m/Tl_c (i.e., ratio of Tl concentrations in mantle peridotite (m) to contaminants) that can produce the mantle-like $\varepsilon^{205}Tl$ values in Samples 18JF10 and 18JF44 should be higher than ∼10. The SCLM beneath the NCC experienced significant modification in the Mesozoic due to the delamination and/or thermal erosion occurring in the Mesozoic and became re-enriched, which might have increased the Tl_m/Tl_c ratio in the source of the Early Cretaceous LJ volcanic rocks (e.g., Foley, 2008; Gao et al., 2004; Xu, 2001; Yang et al., 2008; Zhang, 2005; Zhang et al., 2002, 2003). More importantly, Tl is proposed to be fluid-mobile in arc settings (Noll et al., 1996). Nielsen et al. (2009) proposed a significant Tl-loss, with an upper limit of 90%, could occur due to the dehydration process during the oceanic crust subduction. Such a Tl-loss can also increase the Tl_m/Tl_c ratio and dilute the fractionated Tl isotopic signature from the low-T AOC in the metasomatic agents for the source of the Early Cretaceous LJ volcanic rocks. Thus, it is likely that Tl loss during slab dehydration can lead to the insignificant effects of low-T AOC on the Tl isotopic composition in the source of the LJ volcanic rocks.

5. Conclusions

In this study, we performed the first Tl isotope measurements in alkaline rocks to explore whether Tl isotopes can effectively constrain the nature of metasomatic agents for the SCLM. Samples from the Hekanzi and Saima alkaline complexes have Tl isotope compositions identical to the modern upper mantle, suggesting that low-T AOC and pelagic sediments are unlikely to be important components in the metasomatic agents for the sources of the Hekanzi and Saima alkaline complexes. These findings reconcile with previous O-Nd-Hf isotope studies and the tectonic context, that is, southward subduction of the paleo–Asian Ocean plate and northward subduction of the Yangtze continental crust beneath the NCC during the late Paleozoic to early Mesozoic. Most Early Cretaceous LJ volcanic rocks have mantle-like $\varepsilon^{205}Tl$ values. The combined O-Nd-Hf-Tl isotope data indicate that the metasomatic agent for the source of LJ volcanics might originate from low-T AOC with an extremely low Tl concentration resulting from dehydration process during the oceanic crust subduction. Our Tl isotope data provide complementary constrains to the Sr-Nd-Hf-O isotopes on the nature of metasomatic agent in the subcontinental lithospheric mantle. However, characteristic Tl isotopic composition reflecting the presence of low-T AOC and pelagic sediments in the metasomatic agents for the SCLM is still lacking. Much work is still required to ascertain the Tl cycle of the Earth and further make Tl isotopes a powerful tool to trace recycled materials in the SCLM.

Acknowledgments
We thank Sean Newby for the help with Tl isotope measurements. We thank two anonymous reviewers for their constructive reviews and Lucy Flesch for handling the manuscript. This work was supported by the National Natural Science Foundation of China (42103011, 41688103, and 41702059), National Key R&D Program of China (2016YFC0600109). JDO would like to thank the National Science Foundation (EAR-2026926), National Aeronautics and Space Administration (80NSSC18K1532), Sloan Foundation (FG-2020–13552) for funding the elemental work and a portion of this work was performed at the National High Magnetic Field Laboratory in Tallahassee, Florida, which is supported by National Science Foundation Cooperative Agreement No. DMR-1644779 and by the State of Florida.

Data Availability Statement

Our data is available in Table 1 and online (http://doi.org/10.5281/zenodo.6059272).

References

Aarons, S. M., Johnson, A. C., & Rader, S. T. (2021). Forming Earth's continental crust: A Nontraditional stable isotope perspective. *Elements*, *17*(6), 413–418. https://doi.org/10.2138/gselements.17.6.413

Baker, R. G. A., Rehkämper, M., Ihlenfeld, C., Oates, C. J., & Coggon, R. (2010). Thallium isotope variations in an ore-bearing continental igneous setting: Collahuasi formation, northern Chile. *Geochimica et Cosmochimica Acta*, *74*(15), 4405–4416. https://doi.org/10.1016/j.gca.2010.04.068

Coltorti, M., Beccaluva, L., Bonadiman, C., Salvini, L., & Siena, F. (2000). Glasses in mantle xenoliths as geochemical indicators of metasomatic agents. *Earth and Planetary Science Letters*, *183*(1–2), 303–320. https://doi.org/10.1016/s0012-821x(00)00274-0

Eiler, J. M. (2001). Oxygen isotope variations of basaltic lavas and upper mantle rocks. *Reviews in Mineralogy and Geochemistry*, *43*(1), 319–364. https://doi.org/10.2138/gsrmg.43.1.319

Feng, Y., Yang, J., Sun, J., & Zhang, J. (2020). Material records for Mesozoic destruction of the North China craton by subduction of the Paleo-Pacific slab. *Science China Earth Sciences*, *63*(5), 690–700. https://doi.org/10.1007/s11430-019-9564-4

Foley, S. F. (2008). Rejuvenation and erosion of the cratonic lithosphere. *Nature Geoscience*, *1*(8), 503–510. https://doi.org/10.1038/ngeo261

Gao, S., Rudnick, R. L., Yuan, H.-L., Liu, X.-M., Liu, Y.-S., Xu, W.-L., et al. (2004). Recycling lower continental crust in the North China craton. *Nature*, *432*(7019), 892–897. https://doi.org/10.1038/nature03162

Gaschnig, R. M., Rader, S. T., Reinhard, C. T., Owens, J. D., Planavsky, N., Wang, X., et al. (2021). Behavior of the Mo, Tl, and U isotope systems during differentiation in the Kilauea IKI lava lake. *Chemical Geology*, *574*, 120239. https://doi.org/10.1016/j.chemgeo.2021.120239

Gregory, R. T., & Taylor, H. P. (1981). An oxygen isotope profile in a section of Cretaceous oceanic crust, Samail Ophiolite, Oman: Evidence for $\delta^{18}O$ buffering of the oceans by deep (>5 km) seawater-hydrothermal circulation at mid-ocean ridges. *Journal of Geophysical Research*, *86*(B4), 2737–2755. https://doi.org/10.1029/jb086ib04p02737

Griffin, W. L., Pearson, N. J., Belousova, E., Jackson, S. E., van Achterbergh, E., O'Reilly, S. Y., & Shee, S. R. (2000). The Hf isotope composition of cratonic mantle: LAM-MC-ICPMS analysis of zircon megacrysts in kimberlites. *Geochimica et Cosmochimica Acta*, *64*(1), 133–147. https://doi.org/10.1016/S0016-7037(99)00343-9

Jordan, T. H. (1978). Composition and development of the continental tectosphere. *Nature*, *274*(5671), 544–548. https://doi.org/10.1038/274544a0

Nielsen, S. G., Klein, F., Kading, T., Blusztajn, J., & Wickham, K. (2015). Thallium as a tracer of fluid-rock interaction in the shallow Mariana Forearc. *Earth and Planetary Science Letters*, *430*, 416–426. https://doi.org/10.1016/j.epsl.2015.09.001

Nielsen, S. G., Prytulak, J., Blusztajn, J., Shu, Y., Auro, M., Regelous, M., & Walker, J. (2017). Thallium isotopes as tracers of recycled materials in subduction zones: Review and new data for lavas from Tonga-Kermadec and Central America. *Journal of Volcanology and Geothermal Research*, *339*, 23–40. https://doi.org/10.1016/j.jvolgeores.2017.04.024

Nielsen, S. G., Rehkämper, M., Baker, J., & Halliday, A. N. (2004). The precise and accurate determination of thallium isotope compositions and concentrations for water samples by MC-ICPMS. *Chemical Geology*, *204*(1–2), 109–124. https://doi.org/10.1016/j.chemgeo.2003.11.006

Nielsen, S. G., Rehkämper, M., Brandon, A. D., Norman, M. D., Turner, S., & O'Reilly, S. Y. (2007). Thallium isotopes in Iceland and Azores lavas—Implications for the role of altered crust and mantle geochemistry. *Earth and Planetary Science Letters*, *264*(1–2), 332–345. https://doi.org/10.1016/j.epsl.2007.10.008

Nielsen, S. G., Rehkämper, M., Norman, M. D., Halliday, A. N., & Harrison, D. (2006). Thallium isotopic evidence for ferromanganese sediments in the mantle source of Hawaiian basalts. *Nature*, *439*(7074), 314–317. https://doi.org/10.1038/nature04450

Nielsen, S. G., Rehkämper, M., Porcelli, D., Andersson, P., Halliday, A. N., Swarzenski, P. W., et al. (2005). Thallium isotope composition of the upper continental crust and rivers—An investigation of the continental sources of dissolved marine thallium. *Geochimica et Cosmochimica Acta*, *69*(8), 2007–2019. https://doi.org/10.1016/j.gca.2004.10.025

Nielsen, S. G., Rehkämper, M., & Prytulak, J. (2017). Investigation and application of thallium isotope fractionation. *Reviews in Mineralogy and Geochemistry*, *82*(1), 759–798. https://doi.org/10.2138/rmg.2017.82.18

Nielsen, S. G., Rehkämper, M., Teagle, D. A. H., Butterfield, D. A., Alt, J. C., & Halliday, A. N. (2006). Hydrothermal fluid fluxes calculated from the isotopic mass balance of thallium in the ocean crust. *Earth and Planetary Science Letters*, *251*(1–2), 120–133. https://doi.org/10.1016/j.epsl.2006.09.002

Nielsen, S. G., Shimizu, N., Lee, C.-T. A., & Behn, M. D. (2014). Chalcophile behavior of thallium during MORB melting and implications for the sulfur content of the mantle. *Geochemistry, Geophysics, Geosystems*, *15*(12), 4905–4919. https://doi.org/10.1002/2014gc005536

Nielsen, S. G., Shu, Y., Wood, B. J., Blusztajn, J., Auro, M., Norris, C. A., & Wörner, G. (2021). Thallium isotope fractionation during magma degassing: Evidence from experiments and Kamchatka arc lavas. *Geochemistry, Geophysics, Geosystems*, *22*(5), e2020GC009608. https://doi.org/10.1029/2020gc009608

Nielsen, S. G., Williams, H. M., Griffin, W. L., O'Reilly, S. Y., Pearson, N., & Viljoen, F. (2009). Thallium isotopes as a potential tracer for the origin of cratonic eclogites. *Geochimica et Cosmochimica Acta*, *73*(24), 7387–7398. https://doi.org/10.1016/j.gca.2009.09.001

Nielsen, S. G., Yogodzinski, G., Prytulak, J., Plank, T., Kay, S. M., Kay, R. W., et al. (2016). Tracking along-arc sediment inputs to the Aleutian arc using thallium isotopes. *Geochimica et Cosmochimica Acta*, *181*, 217–237. https://doi.org/10.1016/j.gca.2016.03.010

Noll, P. D., Newsom, H. E., Leeman, W. P., & Ryan, J. G. (1996). The role of hydrothermal fluids in the production of subduction zone magmas: Evidence from siderophile and chalcophile trace elements and boron. *Geochimica et Cosmochimica Acta*, *60*(4), 587–611. https://doi.org/10.1016/0016-7037(95)00405-X

Owens, J. D. (2019). *Application of thallium isotopes: Tracking marine oxygenation through manganese oxide burial*. Cambridge University Press. Retrieved from https://doi.org/10.1017/9781108688697

Prouteau, G., Scaillet, B., Pichavant, M., & Maury, R. (2001). Evidence for mantle metasomatism by hydrous silicic melts derived from subducted oceanic crust. *Nature*, *410*(6825), 197–200. https://doi.org/10.1038/35065583

Prytulak, J., Brett, A., Webb, M., Plank, T., Rehkämper, M., Savage, P. S., & Woodhead, J. (2017). Thallium elemental behavior and stable isotope fractionation during magmatic processes. *Chemical Geology*, *448*, 71–83. https://doi.org/10.1016/j.chemgeo.2016.11.007

Rader, S. T., Gaschnig, R. M., Newby, S. M., Bebout, G. E., Mirakian, M. J., & Owens, J. D. (2021). Thallium behavior during high-pressure metamorphism in the Western Alps, Europe. *Chemical Geology*, *579*, 120349. https://doi.org/10.1016/j.chemgeo.2021.120349

Rehkämper, M., Frank, M., Hein, J. R., & Halliday, A. (2004). Cenozoic marine geochemistry of thallium deduced from isotopic studies of Ferro-manganese crusts and pelagic sediments. *Earth and Planetary Science Letters*, *219*(1–2), 77–91. https://doi.org/10.1016/s0012-821x(03)00703-9

Rudnick, R. L., & Gao, S. (2003). Composition of the continental crust. In H. D. Holland & K. K. Turekian (Eds.) (Vol. *3*, pp. 1–64). Elsevier-Pergamon. https://doi.org/10.1016/b0-08-043751-6/03016-4

Shu, Y., Nielsen, S. G., Marschall, H. R., John, T., Blusztajn, J., & Auro, M. (2019). Closing the loop: Subducted eclogites match thallium isotope compositions of ocean island basalts. *Geochimica et Cosmochimica Acta*, *250*, 130–148. https://doi.org/10.1016/j.gca.2019.02.004

Shu, Y., Nielsen, S. G., Zeng, Z., Shinjo, R., Blusztajn, J., Wang, X., & Chen, S. (2017). Tracing subducted sediment inputs to the Ryukyu arc-Okinawa trough system: Evidence from thallium isotopes. *Geochimica et Cosmochimica Acta*, *217*, 462–491. https://doi.org/10.1016/j.gca.2017.08.035

Tappe, S., Pearson, D. G., Kjarsgaard, B. A., Nowell, G., & Dowall, D. (2013). Mantle transition zone input to kimberlite magmatism near a subduction zone: Origin of anomalous Nd–Hf isotope systematics at Lac de Gras, Canada. *Earth and Planetary Science Letters*, *371–372*, 235–251. https://doi.org/10.1016/j.epsl.2013.03.039

Valley, J. W., Kinny, P. D., Schulze, D. J., & Spicuzza, M. J. (1998). Zircon megacrysts from kimberlite: Oxygen isotope variability among mantle melts. *Contributions to Mineralogy and Petrology*, *133*(1–2), 1–11. https://doi.org/10.1007/s004100050432

Vervoort, J. D., Plank, T., & Prytulak, J. (2011). The Hf–Nd isotopic composition of marine sediments. *Geochimica et Cosmochimica Acta*, *75*(20), 5903–5926. https://doi.org/10.1016/j.gca.2011.07.046

Wang, H. Z., & Mo, X. X. (1995). An outline of the tectonic evolution of China. *Episodes*, *18*(1–2), 6–16. https://doi.org/10.18814/epiiugs/1995/v18i1.2/003

Wu, F. Y., Yang, J. H., Xu, Y. G., Wilde, S. A., & Walker, R. J. (2019). Destruction of the North China craton in the Mesozoic. *Annual Review of Earth and Planetary Sciences*, *47*(1), 173–195. https://doi.org/10.1146/annurev-earth-053018-060342

Xu, Y. G. (2001). Thermo-tectonic destruction of the Archaean lithospheric keel beneath the Sino-Korean craton in China: Evidence, timing and mechanism. *Physics and Chemistry of the Earth—Part A: Solid Earth and Geodesy*, *26*(9–10), 747–757. https://doi.org/10.1016/S1464-1895(01)00124-7

Yang, J. H., O'Reilly, S., Walker, R. J., Griffin, W., Wu, F. Y., Zhang, M., & Pearson, N. (2010). Diachronous decratonization of the Sino-Korean craton: Geochemistry of mantle xenoliths from North Korea. *Geology*, *38*(9), 799–802. https://doi.org/10.1130/G30944.1

Yang, J. H., Sun, J. F., Zhang, M., Wu, F. Y., & Wilde, S. A. (2012). Petrogenesis of silica-saturated and silica-undersaturated syenites in the northern North China Craton related to post-collisional and intraplate extension. *Chemical Geology*, *328*, 149–167. https://doi.org/10.1016/j.chemgeo.2011.09.011

Yang, J. H., Wu, F. Y., Wilde, S. A., Belousova, E., & Griffin, W. L. (2008). Mesozoic decratonization of the North China block. *Geology*, *36*(6), 467–470. https://doi.org/10.1130/G24518A.1

Zhang, H. F. (2005). Transformation of lithospheric mantle through peridotite-melt reaction: A case of Sino-Korean craton. *Earth and Planetary Science Letters*, *237*(3–4), 768–780. https://doi.org/10.1016/j.epsl.2005.06.041

Zhang, H. F., Sun, M., Zhou, X. H., Fan, W. M., Zhai, M. G., & Yin, J. F. (2002). Mesozoic lithosphere destruction beneath the North China craton: Evidence from major-trace-element and Sr–Nd–Pb isotope studies of Fangcheng basalts. *Contributions to Mineralogy and Petrology*, *144*(2), 241–254. https://doi.org/10.1007/s00410-002-0395-0

Zhang, H. F., Sun, M., Zhou, X. H., Zhou, M. F., Fan, W. M., & Zheng, J. P. (2003). Secular evolution of the lithosphere beneath the eastern North China craton: Evidence from Mesozoic basalts and high-Mg andesites. *Geochimica et Cosmochimica Acta*, *67*(22), 4373–4387. https://doi.org/10.1016/S0016-7037(03)00377-6

Zhao, G. C., Sun, M., Wilde, S. A., & Li, S. Z. (2005). Late Archaean to palaeoproterozoic evolution of the North China craton: Key issues revisited. *Precambrian Research*, *136*(2), 177–202. https://doi.org/10.1016/j.precamres.2004.10.002

Zheng, J. P. (1999). *Mesozoic-cenozoic mantle replacement and lithospheric thinning beneath eastern China*. China University of Geosciences Press.

Zheng, Y. F. (2012). Metamorphic chemical geodynamics in continental subduction zones. *Chemical Geology*, *328*, 5–48. https://doi.org/10.1016/j.chemgeo.2012.02.005

Zhu, Y. S., Yang, J. H., Sun, J. F., & Wang, H. (2017). Zircon Hf-O isotope evidence for recycled oceanic and continental crust in the sources of alkaline rocks. *Geology*, *45*(5), 407–410. https://doi.org/10.1130/G38872.1

Zhu, Y. S., Yang, J. H., Sun, J. F., Zhang, J. H., & Wu, F. Y. (2016). Petrogenesis of coeval silica-saturated and silica-undersaturated alkaline rocks: Mineralogical and geochemical evidence from the Saima alkaline complex, NE China. *Journal of Asian Earth Sciences*, *117*, 184–207. https://doi.org/10.1016/j.jseaes.2015.12.014